RESEARCH ARTICLE

Medinformatics 2025, Vol. 2(4) 288–298

DOI: 10.47852/bonviewMEDIN52024568



Computer-Aided Drug Design Identifies Amentoflavone as Novel RAB10 Inhibitor: Unlocking New Horizons in Hepatocellular Carcinoma Therapy

Md. Anayet Ullah¹, Priya Paul¹, Sadia Afrin Runa², Fatema Tuz Johura³, Mahafujul Islam Quadery Tonmoy^{3,4}, Md. Shahriar Kabir Shakil^{3,4}, Rumana Rashid⁵ , Md. Mizanur Rahaman^{4,6} and Newaz Mohammed Bahadur^{4,7,*}

Abstract: Hepatocellular carcinoma (HCC) is the most common type of primary liver cancer and is often associated with a poor prognosis, contributing significantly to cancer-related mortalities. It has been established that RAB10, a member of the RAS family, is overexpressed in HCC and plays an oncogenic role in the emergence of HCC, and developing medications that target it may offer a fresh approach to the disease's management. Therefore, a computational approach was employed to identify potential novel RAB10 inhibitors, and 2569 natural compounds were looked into for this. Initially, 10 compounds were identified by virtual screening and molecular docking to have the highest binding affinities (-9.6 to -10.1 kcal/mol) to the active site of RAB10, where 8 were deemed to meet the necessary criteria for becoming a drug-like substance. Following ADMET analysis, Amentoflavone, among the 8 substances, showed a considerable pharmacokinetics index without any associated toxicity. Amentoflavone was found to form both covalent and non-covalent interactions with the active residues of RAB10, essential for inhibiting its activity. LYS154, ALA153, and LYS22 amino acids of RAB10 were found to interact with the Amentoflavone via the generation of three intermolecular H-bonds. The drug-protein combination, which supports maintaining its structural stability and stiffness, demonstrates structural compactness and minimal conformational fluctuation, according to molecular dynamics simulation. Molecular Mechanics Poisson-Boltzmann Surface Area analysis further confirmed the stable binding of Amentoflavone inside the binding pocket of RAB10. These findings hypothesize that Amentoflavone might be a potential RAB10 inhibitor, which would increase HCC's therapeutic prospects.

Keywords: hepatocellular carcinoma, RAB10, Amentoflavone, ADME, natural compounds

1. Introduction

Hepatocellular carcinoma (HCC), also referred to as malignant hepatoma, stands as the most prevalent form of primary liver cancer and is a substantial contributor to cancer-related mortality globally. HCC ranks as the sixth most common malignancy globally, with over 841,000 new cases annually, highlighting its significance as

a pressing public health concern [1–3]. HCC has a grim prognosis, as the 5-year survival rate is only 11% [4, 5]. Despite advancements in various treatment modalities, including surgical interventions, liver-directed therapies, and systemic treatments, the prognosis of HCC has not significantly improved in recent years due to its high potential for metastasis and recurrence. Late-stage diagnosis makes the treatment of HCC more difficult and can make routine surgical treatments challenging [6–8]. Considering these challenges, there is an urgent need to unravel the molecular pathways that propel the development of HCC,

¹Department of Applied Chemistry and Chemical Engineering, Noakhali Science and Technology University, Bangladesh

²Department of Biotechnology and Genetic Engineering, Gopalganj Science and Technology University, Bangladesh

³Department of Biotechnology & Genetic Engineering, Noakhali Science and Technology University, Bangladesh

⁴Computational Biology and Chemistry Lab, Noakhali Science and Technology University, Bangladesh

⁵Department of Public Health Nutrition, Primeasia University, Bangladesh

⁶Department of Microbiology, University of Dhaka, Bangladesh

⁷Department of Chemistry, Noakhali Science and Technology University, Bangladesh

^{*}Corresponding author: Newaz Mohammed Bahadur, Computational Biology and Chemistry Lab and Department of Chemistry, Noakhali Science and Technology University, Bangladesh. Email: nmbahadur@nstu.edu.bd

[©] The Author(s) 2025. Published by BON VIEW PUBLISHING PTE. LTD. This is an open access article under the CC BY License (https://creativecommons.org/licenses/by/4.0/).

identify prognostic markers, and explore novel treatment targets to improve patient outcomes [5].

Targeted therapy is a precision medicine approach that shows promise in cancer treatment by specifically targeting genes or proteins associated with cancer development [9, 10]. Such therapies target biomarkers, which are often aberrantly expressed genes or proteins specific to certain malignancies. Targeted therapies have shown efficacy in selectively eliminating cancer cells while safeguarding healthy, non-cancerous cells [11, 12]. A limited number of targeted therapies for HCC have been approved, which highlights the need to identify new and effective molecular targets and promotes the development of targeted treatment approaches for HCC [5].

Among the promising candidates for treating HCC, the protein-coding gene RAB10 has recently garnered attention. The gene RAB10 is responsible for encoding the RAB10 protein, which possesses GDP and GTP binding domains. It belongs to the RAS superfamily of small GTPases, which is well-known for its participation in a wide range of cellular processes [13–15]. RAB10 has a critical function in controlling the survival and growth of cells, impacting many oncogenic, cellular stress, and apoptotic pathways. Importantly, recent research has identified an overexpression of RAB10 in several liver cancer tissues. Moreover, increased levels of RAB10 in HCC cells have been linked to an unfavorable prognosis for individuals with HCC. The findings established that the RAB10 knockdown brought the expected results – reduced HCC cell proliferation and colony formation; thus, it may be a potential target in HCC [5, 16, 17].

In the contemporary landscape of drug discovery, computational techniques are frequently used to virtually scan large datasets containing a wide range of chemical compounds, including drug-like molecules, natural chemicals, synthesized compounds, and hypothetical molecules. This approach is useful for identifying compounds that may be bioactive and for effectively optimizing those that have a higher affinity for the target receptors. This method thereby simplifies the drug design process, cutting down on processes and related costs [18, 19]. Various molecular modeling and docking approaches are increasingly gaining popularity in efforts to elucidate the quantitative relationship between macromolecule structure and

function, as well as in the development of structure-based drugs [20, 21]. The integration of computational approaches with in vitro studies facilitates the comprehensive evaluation of lead compounds. This includes assessing their inhibitory properties, drug-likeness, pharmacokinetics (PK), and physicochemical characteristics. This combined approach simplifies the process of identifying bioactive molecules with favorable attributes, thereby aiding in the discovery of strong drug candidates for further research [22–25]. Molecular dynamics (MD) simulation is increasingly crucial in structure-based drug design as it serves as a valuable tool for comprehending how receptor-ligand complexes behave in simulated physiological conditions [26].

This current study employs a combination of structure-based molecular docking and virtual screening techniques to identify novel inhibitors for RAB10 and subsequently conducts an investigation into ADMET (absorption, distribution, metabolism, excretion, and toxicity) characteristics of the discovered compounds. Finally, MD simulation is used to evaluate the stability of the drugprotein complex under artificial physiological conditions, providing valuable aspects of the dynamic behavior of this complex. This integrative approach holds promise in uncovering novel therapeutic candidates for targeted therapy in HCC.

2. Methods

A summary of the workflow used in this study for the identification of inhibitors against the target protein RAB10 is presented in Figure 1.

2.1. Protein structure preparation

The 3D structure of the RAB10 protein was required, and it was retrieved from the RCSB-PDB [27] with PDB accession 5SZJ [28]. The structure contains A and B chains, where the A chain represents the RAB10 protein structure (200 amino acids) and the X-ray resolution of this structure is 2.66Å. According to the report in RCSB-PDB, 0% of residues are present in Ramachandran outliers with a clashscore of 6. As the RAB10 protein is located within the A chain, all other entities were removed from the 5SZJ

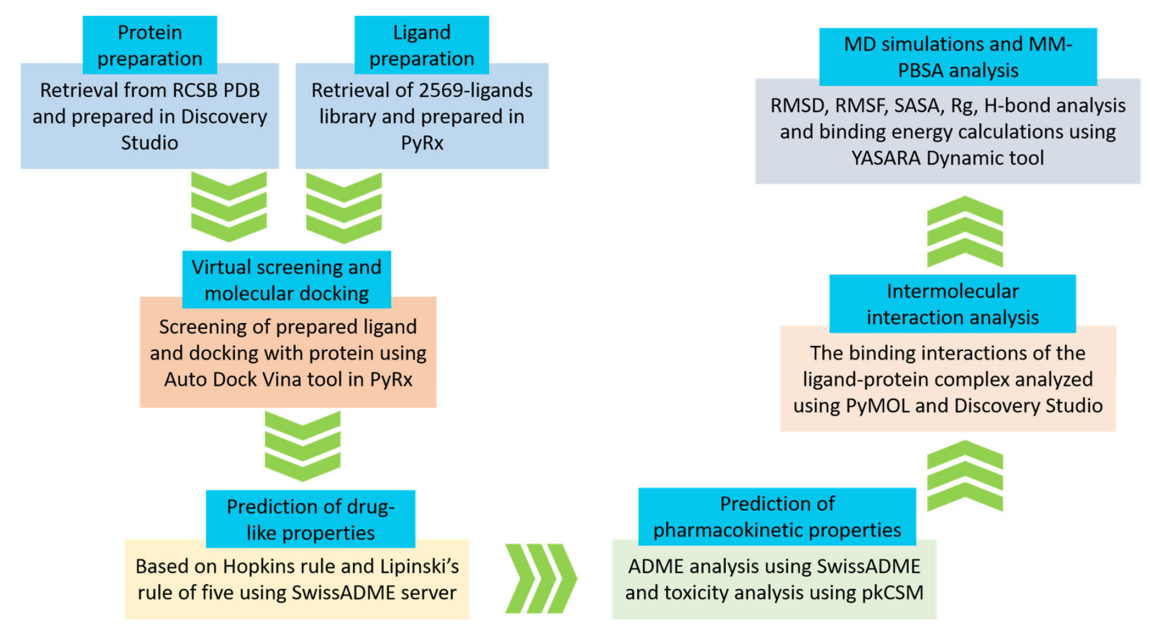


Figure 1. Flowchart depicting the overall workflow of the present study

structure except for the A chain. Moreover, for the docking procedure water molecules were removed from the prepared protein structure, Kollman charges and polar hydrogens were added [29], and finally, YASARA Energy Minimization Server was used to perform energy minimization of the protein structure using the YASARA force field [30, 31].

2.2. Ligand structure preparation

A total of 2569 bioactive natural compounds were retrieved from the Selleckchem natural product library (https://www.selle ckchem.com/screening/natural-product-library.html) and utilized as small molecules (ligand). Among 2569, 357 compounds are used in the field of microbiology. 277, 217, 152, and 88 compounds are used in immunology & inflammation, metabolism, neuronal signaling, and DNA repair, respectively. Moreover, compounds from this collection are employed in endocrinology, apoptosis, angiogenesis, epigenetics, transmembrane transporters, cell cycle, autophagy, and cytoskeletal signaling. The retrieved library containing 2569 natural compounds was imported into PyRx software [32]. The ligands' structure was then given a Gasteiger charge. The Conjugate Gradients algorithm was employed to enforce the Universal Force Field on the ligands' structure to minimize the energy [33]. Each compound's energy minimization process was limited to 200 steps, and it was defined that it would end if the energy difference fell below 0.1 kcal/mol [26].

2.3. Structure-based virtual screening and protein-ligand docking

The structure-based virtual screening based on molecular docking was conducted using the AutoDock Vina tool within the PyRx software [34]. In this process, the previously prepared 3D structure of the RAB10 protein served as the receptor, while the 2569 natural compounds' structures, also previously prepared, were used as ligands. Specific grid dimensions (Å): size (X, Y, Z: 44.3198, 39.0151, 53.5912) and center (X, Y, Z: 23.8246, 21.6033, -42.5035) were set to cover the entire protein by the grid box. The exhaustiveness parameter was set to 8 for each ligand in order to produce 8 low-energy conformers binding to the receptor. Every docking operation used the same initialization to provide reproducible docking outcomes. Additionally, the same parameters were utilized across all docking operations to further guarantee consistency and reproducibility in the results.

2.4. Prediction of drug-like properties

To assess the drug-like characteristics of ligands (natural compounds) with the highest affinity for binding to the receptor (RAB10), the SwissADME web server [35] was utilized. Following the principles outlined by Bickerton et al. [36] and Lipinski [37], the drug-likeness characteristics of these ligands were investigated. The "rule of five" proposed by Lipinski is a method used to assess whether a substance has favorable oral absorption characteristics or not. The "rule of five" is satisfied by a chemical with the following properties: a molecular weight (MW) less than 500 daltons (Da), an octanol-water partition coefficient (iLOGP) less than 5, no more than 5 hydrogen bond donors, and no more than 10 hydrogen bond acceptors. The "QED concept," proposed by Hopkins adds four more physicochemical features to Lipinski's four. These additional characteristics include TPSA (topological polar surface area), which should range from 20 to 130, the number of heavy atoms, which should range from 15 to 50, the number of rotatable bonds, which should range from 0 to 5, and the absence of PAINS and Brenk alerts for unwanted components. Natural compounds satisfying both Hopkins' "QED concept" and Lipinski's "rule of five" were classified as drug-like compounds. It is important to note that some substances are utilized in clinical settings despite not meeting all of these requirements [26].

2.5. Prediction of PK properties

Before deciding to advance a drug candidate, a comprehensive assessment of its PK features is conducted. This examination includes aspects like ADMET. The SwissADME is a free online tool that allows users to analyze a variety of parameters, including the absorption, distribution, metabolism, and excretion (ADME) characteristics of the chosen drug-like molecules. This tool employs multiple methods, including BOILED Egg, and iLOGP, to predict diverse PKs, physicochemical features, and medicinal chemistry aspects [38]. Boiled egg method is used to predict two essential ADME parameters gastrointestinal absorption (GI) and blood-brain barrier (BBB) [39]. iLOGP indicates the n-octanol/water partition coefficient which is a conventional descriptor for lipophilicity [40]. Using a web-based server called pkCSM [40], the toxicity levels of the chosen drug-like substances were assessed. For our investigation, we took into account the following ADMET properties: GI absorption, water solubility, skin permeation, and P-glycoprotein substrate are properties of absorption. Distribution properties include the steady-state volume of distribution (VDss), and BBB permeability. Excretion (drug total clearance), metabolism (CYP2D6/CYP3A4 substrate and CYP2D6 inhibitor), and toxicity (skin sensitization, hERG channel inhibitor I, hepatotoxicity, T. pyriformis toxicity, and AMES toxicity) were considered.

2.6. Intermolecular interaction analysis

The promising ligands from the ADMET analysis bound to the RAB10 protein's pre-optimized modeling structure were utilized through PyMOL and Discovery Studio to examine their intermolecular interaction. PyMOL facilitates the investigation of protein-ligand interactions by allowing the user to visualize and examine the interactions [41]. Additionally, calculating binding affinity to determine the intensity of the contact, PyMOL can depict the binding modes of the ligands, such as hydrogen bonds, van der Waals, Pi-Sigma, Pi-Pi T-shaped, Amide-Pi Stacked, and Alkyl interactions. To undertake further investigation of the interaction, PyMOL can also measure the separation between certain atoms in the protein and ligand and assess the surface area of the binding pocket [42].

2.7. MD simulation and Molecular Mechanics Poisson-Boltzmann Surface Area (MM-PBSA) calculation

To investigate the stability of the interaction between potential therapeutic chemicals and the target protein, MD simulation is frequently employed [43]. To assess the stability of the drug's binding to the RAB10 protein, we utilized the YASARA Dynamics tool [44] to examine the dynamic behavior of the drug-RAB10 complex over time. The drug-RAB10 complex's structure was cleaned up before the simulation began, followed by the optimization of the complex's hydrogen bond network [45]. Then, using a grid size of (96.9654 × 96.9654 × 96.9654), a virtual cubic box featuring periodic cell boundary conditions was created as the stage for simulation. Inside this box, the AMBER14 force

field [46] was employed to simulate the drug-RAB10 complex, creating a dynamic scenario within a simulated aquatic environment. AMBER 14 is a powerful MD suite designed for simulating biomolecules like proteins, nucleic acids, and lipids. Its ff14SB force field is optimized for accurate protein dynamics. AMBER offers both explicit and implicit solvent models and supports advanced methods like replica exchange (REMD) and accelerated MD (aMD) for enhanced sampling. With parallel computing, it handles large-scale simulations efficiently, making it ideal for protein folding, binding studies, and other biomolecular research [47]. To restore equilibrium, the system introduced sodium and chlorine ions into the cubic box using the TIP3P (transferable intermolecular interaction potential 3 points) method [48]. The energy of the drug-RAB10 structure was then reduced by employing the steepest descent approach. In the YASARA Dynamics software, energy minimization was used to smooth out any irregularities and adjust the structure's covalent geometry [49]. Setting the radius cut-off to 8Å, we computed the short-range Coulomb forces and van der Waals interactions. We then used the Particle Mesh Ewalds technique to compute the longrange Coulomb interactions [50]. The physiological conditions used for all of these computations were measured at 298 K, pH 7.4, and 0.9% NaCl. Subsequently, an MD simulation running for 200 nanoseconds (ns) was performed at a time interval equal to 2.5 femtoseconds (fs) [51, 52]. Following the simulation, the trajectory files were examined to derive a number of metrics, such as RMSD (root mean square deviation), RMSF (root mean square fluctuation), Rg (radius of gyration), SASA (solvent-accessible surface area), and H-bond analysis. The RMSD values are calculated by using the following formula, where Ri is the vector linking the positions of atom i [of N atoms] in the reference snapshot and the current snapshot after optimal superposition:

$$RMSD = \sqrt{\frac{\sum_{i=1}^{n} R_i \times R_i}{n}}$$
 (1)

The RMSF value per solute residue is calculated from the average RMSF of the complex's constituting atoms. The RMSF of atom i with j running from 1 to 3 for the x, y, and z coordinate of the atom position vector P and k running over the set of N evaluated snapshots is given by the following formula:

RMSFi =
$$\sqrt{\sum_{j=1}^{3} \left(\frac{1}{N} \sum_{k=1}^{N} P_{ijk}^{2} - \underline{P}_{ijk}^{2}\right)}$$
 (2)

Radius of gyration, Rg, is calculated by using this formula, where \vec{C} is the center of mass, and \vec{R}_i is the position of atom i of N.

$$Rg = \sqrt{\frac{\sum_{i=1}^{N} Mass_{i} (\vec{R}_{i} - \vec{C})^{2}}{\sum_{i=1}^{N} Mass_{i}}}$$
(3)

The number of hydrogen bonds is calculated by using the bond energy in [kJ/mol] as a function of the Hydrogen-Acceptor distance in [A] and two scaling factors according to the following formula:

EnergyHBO =
$$25 \times \frac{2.6 - max(D_{iSH} - A_r^{2.1})}{0.5} \times Scale_{D-H-A} \times Scale_{H-A-X}$$
 (4)

The first scaling factor depends on the angle formed by the Donor-Hydrogen-Acceptor:

$$Scale_{D-H-A} = \{0 \in range \ 0 - 100 \ degrees \ 0 - 1 \ \in ranges \ 100 - 165 \ degrees \ 1 \ \in ranges \ 165 - 180 \ degrees$$
 (5)

The second scaling factor is determined based on the angle formed by Hydrogen-Acceptor-X, where X represents the atom covalently bound to the acceptor. If X is a heavy atom:

$$Scale_{H-A-x} = \{0 \in range \ 0 - 85 \ degrees \ 0 - 1 \$$
 $\in ranges \ 85 - 95 \ degrees \ 1 \$
 $\in ranges \ 95 - 180 \ degrees$ (6)

If X is a hydrogen, slightly smaller angles are permitted:

$$Scale_{H-A-H} = \{0 \in range\ 0 - 75\ degrees\ 0 - 1 \$$
 $\in ranges\ 75 - 85\ degrees\ 1 \$
 $\in ranges\ 85 - 180\ degrees \$
 (7)

A hydrogen bond is considered present if the hydrogen bond energy calculated using this formula is better than 6.25 kJ/mol.

The binding free energy was then calculated using the MM-PBSA method on all of the trajectory data. The following formula [53] was used to get the binding free energy:

$$\begin{aligned} \text{Binding Free Energy} &= E_{\text{potRecept}} + E_{\text{solvRecept}} + E_{\text{potLigand}} \\ &+ E_{\text{solvLigand}} - E_{\text{potComplex}} - E_{\text{solvComplex}} \end{aligned} \tag{8}$$

where the terms "pot" and "solv" denote the potential and solvation energy, respectively.

3. Results

3.1. Structure-based virtual screening and protein-ligand docking

In the pursuit of identifying potential inhibitors for the RAB10 protein, this study employed a comprehensive structure-based virtual screening and protein-ligand docking analysis. The initial virtual screening encompassed a dataset of 2569 natural compounds, from which 1562 compounds were identified as candidates for binding to the RAB10 protein based on its structure. Subsequently, a thorough molecular docking analysis was performed on these 1562 compounds to evaluate their binding affinities to RAB10 and the findings revealed a subset of 10 natural compounds demonstrating binding affinities within the

Table 1. The binding affinity of the top 10 natural compounds docked onto the RAB10 protein

Ligand	Binding affinity (Kcal/mol)
Epicatechin gallate	-10.1
Coelenterazine	-10
Epigallocatechin gallate	-9.9
Asarinin	-9.9
Amentoflavone	-9.8
FM-381	-9.8
Paliperidone	-9.7
Sennoside B	-9.7
Hederacoside C	-9.6
alpha-Naphthoflavone	-9.6

Table 2. Drug-like properties of the 10 natural compounds

			H-bond	H-bond		Heavy	Rotatable	Alert	
Natural compound	MW (Da)	iLOGP	donors	acceptors	TPSA ($Å^2$)	atoms	bonds	Pains	Brenk
Epicatechin gallate	442.37	1.44	7	10	177.14	32	4	1	1
Coelenterazine	423.46	2.78	3	5	90.88	32	5	0	0
Epigallocatechin gallate	458.37	1.87	8	11	197.37	33	4	1	1
Asarinin	354.35	3.46	0	6	55.38	26	2	0	0
Amentoflavone	538.46	3.06	6	10	181.80	40	3	0	0
FM-381	428.49	3.00	1	5	103.74	32	5	0	2
Paliperidone	426.48	3.86	4	7	84.39	31	4	0	0
Sennoside B	862.74	1.14	12	20	347.96	62	9	0	0
Hederacoside C	1221.38	4.02	15	26	412.82	85	14	0	2
alpha-Naphthoflavone	272.30	2.94	0	2	30.21	21	1	0	1

range of -9.6 to -10.1 kcal/mol (Table 1). Moreover, 12 compounds exhibited binding affinities falling between -9.1 and -9.5 kcal/mol. In contrast, the remaining 1540 compounds exhibited binding affinities below -9.1 kcal/mol. Particularly, epicatechin gallate emerged as a potential candidate, showing the highest binding energy of -10.1 kcal/mol (Table 1).

3.2. Prediction of drug-like properties

The drug-like properties of the chosen 10 natural compounds were explored using a comprehensive approach that integrates both Hopkins' "QED" and Lipinski's "rule of five" concepts. Notably, Sennoside B and Hederacoside C were identified as outliers, failing to meet Lipinski's criteria concerning MW, hydrogen bond acceptors, and hydrogen bond donors, and also lacking adherence to Hopkins' rules regarding TPSA, heavy atoms, rotatable bonds, and undesirable structural alerts (Table 2). In contrast, the remaining 8 compounds displayed a noteworthy alignment with the specified criteria of both "QED" and Lipinski's concepts, positioning them as more promising candidates for drug development (Table 2).

3.3. Prediction of PK properties

The PK assessment of the potential 10 therapeutic candidates was conducted through in silico ADMET analysis and outlined in Table 3. The investigation identified Hederacoside C, Epicatechin gallate, and Epigallocatechin gallate as compounds with suboptimal GI absorption, whereas others demonstrated favorable absorption in the GI system. Pivoting to P-glycoprotein (P-gp) substrates, coelenterazine, FM-381, and paliperidone are identified as P-gp substrate. Apart from absorption, the investigation revealed BBB permeability for select compounds like Asarinin,

and Alpha-Naphthoflavone. However, given their considerable GI absorption and lack of P-gp substrate status, Amentoflavone emerges as the only candidate meeting the specified requirements mentioned above. Despite its modest solubility in water, Amentoflavone displayed higher skin permeability (value > -2.5). The favorable distribution rate, as evidenced by log VDss values (> 0.45 implies higher dispersion), coupled with a promising total clearance score (0.484 ml/min/kg), suggests efficient removal from the body. In terms of metabolism, Amentoflavone proves advantageous as it is not expected to act as a CYP2D6 inhibitor. Additionally, it functions as a substrate for CYP3A4, a notable characteristic (Table 3).

For Amentoflavone, the AMES test, mutagenicity test revealed no concerns, and no negative effects were noted concerning hepatotoxicity, skin sensitivity, or the hERG inhibitor I channel. The T. pyriformis toxicity parameter further supports the compound's safety profile with a value of 0.245. The nominated natural compound, Amentoflavone, whose 2D chemical structure is shown in Figure 2 has the IUPAC designation 8-[5-(5,7-dihydroxy-4-oxochromen-2-yl)-2-hydroxyphenyl]-5,7-dihydroxy-2-(4-hydroxyphenyl)chromen-4-one.

3.4. Intermolecular interaction analysis

Intermolecular interaction analysis was conducted to elucidate the specific molecular interactions between the Amentoflavone molecule and the RAB10 protein, revealing a network of bonds and contacts. Three intermolecular hydrogen bonds were identified, establishing connections between the Amentoflavone molecule and the amino acids LYS154, ALA153, and LYS22 of the RAB10 protein (Figure 3). Furthermore, van der Waals interactions were observed between Amentoflavone and several amino acids, including

Table 3. Pharmacokinetic properties of the 10 selected natural compounds

	Absorption				Distribution		Metabolism		Excretion
	Water			Skin	,			CYP2D6/	Drug total
	solubility		P-gp	permeation	BBB	Log	CYP2D6	CYP3A4	clearance
Natural compound	(mg/ml)	GI absorption	substrate	(cm/s)	permeant	VDss	inhibitor	substrate	(ml/min/kg)
Epicatechin gallate	-3.7	Low (62.096%)	No	-7.91	No	0.664	No	No	-0.169
Coelenterazine	-6.25	High (89.625%)	Yes	-4.95	No	-0.421	Yes	No	0.827
Epigallocatechin gallate	-3.56	Low (47.395%)	Yes	-8.27	No	0.806	No	No	0.292
Asarinin	-3.93	High (97.810%)	No	-6.56	Yes	-0.17	No	No/Yes	-0.126
Amentoflavone	-6.75	High (84.356%)	No	-6.01	No	-1.066	No	No/Yes	0.484
FM-381	-4.54	High (96.839%)	Yes	-6.68	No	0.33	Yes	No	0.638
Paliperidone	-3.95	High (94.350%)	Yes	-7.36	No	1.19	Yes	No/Yes	0.757
alpha-Naphthoflavone	-5.2	High (97.770%)	No	-4.55	Yes	0.073	No	No/Yes	0.413

Figure 2. Chemical structure (2-Dimensional) of Amentoflavone (8-[5-(5,7-dihydroxy-4-oxochromen-2-yl)-2-hydroxyphenyl]-5,7-dihydroxy-2-(4 hydroxyphenyl)chromen-4-one)

ASP125, ASN122, SER152, GLY21, VAL20, GLY19, THR23, and ILE39. Notably, a diverse array of hydrophobic contacts was unveiled, encompassing pi-cation, pi-pi stacking, pi-pi T-shaped, and pi-alkyl interactions. PHE34 engaged in pi-pi T-shaped interactions, while PHE38 participated in pi-pi stacking. LYS123, on the other hand, was found to participate in pi-cation interactions. Furthermore, the

Amentoflavone molecule and the RAB10 protein's CYS24 amino acid exhibited pi-alkyl interactions (Figure 3).

3.5. Molecular dynamic simulation and MM-PBSA analysis

MD simulation was performed to thoroughly analyze the Amentoflavone-RAB10 drug-protein complex and to determine the degree to which it deviates from its initial structural conformation in an artificial physiological condition. Using a 200ns MD simulation, the RMSD was shown to be the most important quantitative measure for identifying structural integrity. The calculated mean RMSD value, expressed as 1.82 Å over the whole simulation period, indicates a considerable level of structural stability. A noticeable deviation from this stability at 160 ns, with an RMSD of 2.27 Å was observed. A zigzag trend in structural deviation was observed up to 10.75 ns, after which the complex demonstrated stability until 17.5 ns. Following a brief period of frame divergence between 17.5 and 18.5 ns, the complex re-stabilized and maintained this condition for the remainder of the simulation (Figure 4(A)).

The RMSF values throughout the simulation period were calculated to figure out the adaptability of the complexes under scrutiny. The results of this analysis revealed a noteworthy trend: the majority of residues demonstrated a commendable level of stability, as minimal fluctuations were observed in their respective RMSF values. Specifically, amino acids MET1, ALA2, and LYS3 manifested a heightened degree of flexibility relative to their counterparts, evidenced by RMSF values ranging from 3.71 to 6.29 Å. In contrast, the amino acids, ranging from 75–175, constituting the surface binding pocket showed a comparatively constrained flexibility profile, consistently maintaining RMSF values below 2.5 Å. The interaction between Amentoflavone and the protein involved the formation of hydrogen bonds with LYS154, ALA153, and LYS22 amino acids, showing RMSF values within the range of 0.82 to 1.51 Å. Furthermore, van der Waals interactions were identified for ASP125, ASN122,

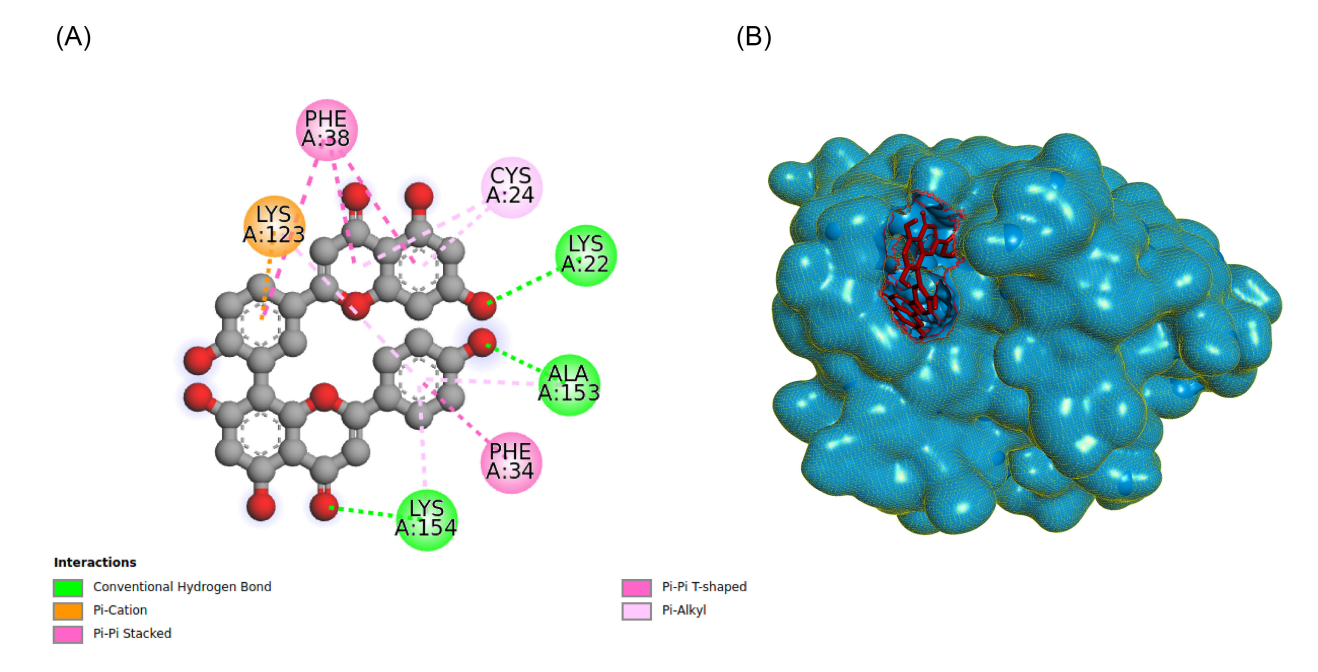


Figure 3. Intermolecular interactions between the RAB10 protein and the Amentoflavone molecule. (A) 2-Dimensional representation of the RAB10-Amentoflavone interaction; (B) 3-Dimensional representation of the docking pose of Amentoflavone with RAB10 protein. RAB10 protein is blue whereas red indicates the Amentoflavone molecule.

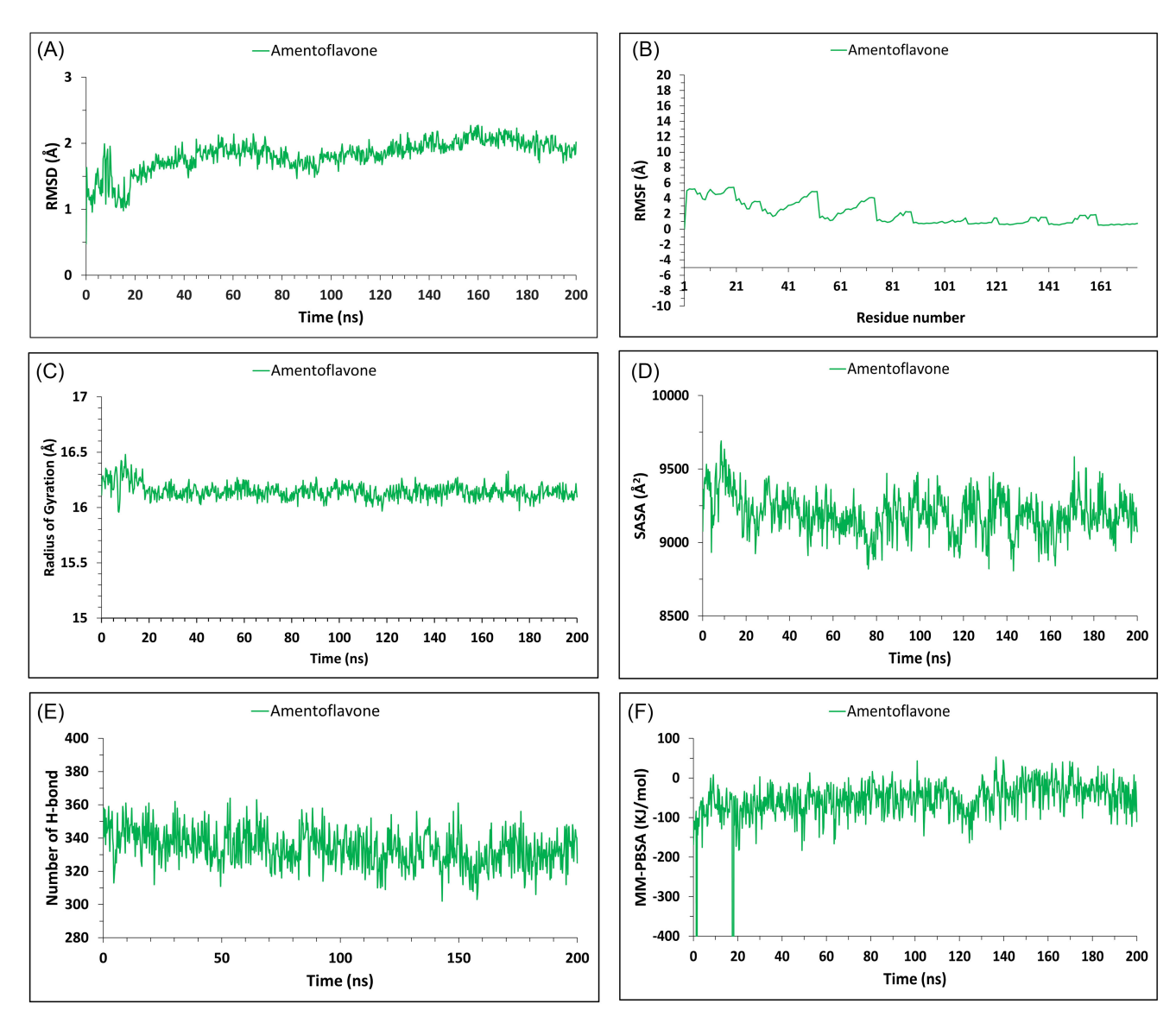


Figure 4. Molecular dynamics (MD) simulation analysis of the Amentoflavone-RAB10 complex over 200 ns. (A) Root mean square deviation (RMSD) showing overall structural stability; (B) root mean square fluctuation (RMSF) indicating residue-level flexibility; (C) radius of gyration representing the compactness of the complex; (D) solvent-accessible surface area (SASA) depicting surface exposure; (E) number of hydrogen bonds formed throughout the simulation; and (F) binding free energy calculated using MM/PBSA, showing the energetic stability of the complex.

SER152, GLY21, VAL20, GLY19, and THR23 amino acids within the complex, manifesting RMSF values ranging from 0.52 to 0.89 Å, whereas ILE39 deviated with a higher RMSF value of 3.23 Å. The remaining bonds exhibited fluctuations ranging from 0.61 to 1.03 Å. Overall, the Amentoflavone-RAB10 complex reported an average RMSF value of 1.33 Å (Figure 4(B)).

The structural attributes of a drug-protein complex were examined through the application of radius of gyration (Rg) analysis. Rg analysis is a quantitative method employed to assess the rigidity and compactness of molecular systems, providing valuable insights into their structural stability. Throughout the simulation, the Rg values of the Amentoflavone-RAB10 complex were found to persist within a narrow range, precisely between 15.95 and 16.48 Å. The consistent Rg range indicates that the complex maintains a sustained level of compactness, demonstrating remarkable stability (Figure 4(C)).

The SASA analysis was performed to examine the solventexposed surface area of the drug-protein complex. At the initiation of the simulation, the Amentoflavone-RAB10 complex manifested a SASA of 9076.14 $\mbox{\ensuremath{\mbox{\mbox{\sc A}}}}^2$. Subsequently, an average surface area of 9195.2 $\mbox{\ensuremath{\mbox{\sc A}}}^2$ was observed, encapsulating the ensemble behavior of the complex in its dynamic interplay with surrounding solvent molecules. Notably, a distinct shift in the behavior of the complex's surface area was observed, which resulted in a terminal value of 9073.91 $\mbox{\ensuremath{\mbox{\sc A}}}^2$ (Figure 4(D)).

Throughout the simulation process, the H-bond count consistently exceeded 302. Quantitatively, the average H-bond count for the Amentoflavone-RAB10 complex was calculated as 337.54 (Figure 4(E)).

The Molecular Mechanics Poisson-Boltzmann Surface Area (MM-PBSA) method was utilized to determine the binding free energy, aiming to unravel the structural modifications induced by the interaction between the Amentoflavone and the RAB10 protein during a 200 ns simulation. The calculated average binding free energy of the Amentoflavone-RAB10 complex,

standing at -58.69 KJ/mol, signifies a distinctly negative binding free energy (Figure 4(F)).

4. Discussion

The exploration of Amentoflavone as a potential therapeutic agent for HCC through a multi-faceted computational approach gives a full picture of its potential in cancer treatment. The study commences by emphasizing the significance of finding novel molecular targets for HCC. This is because current treatment options are not very effective, and there is a high risk of cancer recurrence with this form of cancer [8]. The identification of RAB10 as a potential target is underscored by recent research findings that reveal overexpression of this protein in specific liver cancer tissue samples [5]. By screening a natural chemical library, the current work seeks to discover novel inhibitors of the RAB10 protein, a promising therapeutic target for treating HCC.

The computational aspect of the study implements advanced techniques, notably virtual screening and molecular docking, to explore an extensive library of 2569 natural compounds. The selection of 10 compounds with the highest binding affinities demonstrates a systematic approach to identifying potential drug candidates. The subsequent drug-likeness assessment further refines the selection, narrowing it down to eight compounds where Amentoflavone emerges as the most promising due to its superior drug-like properties.

Amentoflavone stands out by demonstrating high GI absorption and good water solubility. Notably, the compound does not function as a substrate for P-glycoprotein, indicating a favorable profile for drug distribution within the body. The ideal VDss score further supports this, suggesting efficient distribution. However, it is noteworthy that the compound is unable to pass the BBB and is unable to affect the central nervous system. Crucially, the compound demonstrates positive attributes related to metabolism and elimination. As a substrate for the CYP3A4 enzyme, a key player in drug metabolism within the liver, the drug candidate holds the potential for effective processing in the body. Previous in vitro studies have shown that Amentoflavone can inhibit CYP3A4 and CYP2C9, which are critical enzymes involved in drug metabolism [54]. This could lead to drug-drug interactions and altered PKs of co-administered drugs. However, these inhibitory effects were observed at relatively high concentrations, and further in vivo studies are needed to assess the clinical relevance of these findings. Additionally, the absence of anticipated hindrance to CYP2D6 enzyme activity is a significant advantage, implying that the drug is unlikely to interfere with the metabolism of other drugs that depend on this enzyme. This thorough examination of the compound's PK properties lays a robust foundation for its potential as a drug candidate. Safety considerations, a fundamental aspect of drug development, are comprehensively addressed in the study. Amentoflavone's safety profile emerges as favorable, with no observed issues related to critical factors such as mutagenicity, hERG channel inhibition, skin sensitization, and hepatotoxicity. This thorough evaluation strengthens Amentoflavone's potential suitability and provides confidence in its potential for further development into a feasible therapeutic agent. The study advances into the realm of MD simulation, providing a detailed exploration of the stability and integrity of the Amentoflavone-RAB10 complex. The persistent negative binding free energy observed throughout the simulation signifies a stable interaction between Amentoflavone and RAB10. The average RMSD values of the complex are calculated as 1.82 Å which signifies a high degree of stability and integrity for the complex. Notably, the RMSD profile from the complex did not exceed 2.27 Å emphasizing its overall stability. This is reinforced by a residual fluctuation rate of less than 1.5 Å, indicating minimal deviation from the stable state. The stability of the H-bond adds another layer of confidence in the drug-protein complex. The formation of an H-bond involving LYS154, ALA153, and LYS22 molecules with the therapeutic candidate suggests a stable interaction. The drug, characterized by a fluctuation rate of less than 2.5 Å, demonstrates consistency in the binding pocket. Examining the rigidity and compactness of the drug-protein complex, the Rg value remaining within the range of 15.95 Å to 16.48 Å throughout the simulation is indicative of the complex retaining its initial conformation. This consistency further supports the structural stability observed earlier. Remarkably, the SASA of the drug-protein complex exhibits minimal change from its original condition, emphasizing the robust nature of the complex during the simulation. This computational exploration enhances the understanding of the dynamic interaction between Amentoflavone and RAB10, providing additional scientific insight into its potential as a promising therapeutic candidate. An in vivo study in SK-Hep1/ luc2 tumor-bearing mice found that Amentoflavone suppresses HCC progression by inhibiting ERK/NF-KB activation [55]. Additionally, Amentoflavone can be used in combination with other drugs to achieve a synergistic effect. It has been shown to sensitize HCC cells to sorafenib by inhibiting the expression of sorafenib-induced anti-apoptotic proteins such as XIAP, Mcl-1, and C-FLIP and enhancing sorafenib-induced apoptosis through both extrinsic and intrinsic pathways [56].

The findings of this study highlight Amentoflavone's potential as a therapeutic agent for HCC by targeting the RAB10 protein. The comprehensive computational analysis, combined with insights from previous research, provides a strong foundation for future experimental validation, including in vitro and in vivo studies. These next steps are essential to fully understand the therapeutic efficacy of Amentoflavone and its potential application in clinical settings.

5. Conclusion

This comprehensive computational study provides compelling evidence supporting the potential of Amentoflavone as a promising therapeutic agent for HCC through targeted interaction with the RAB10 protein. While previous studies have identified Amentoflavone's role in inhibiting HCC progression through other pathways, this research expands the scientific understanding by demonstrating its strong and stable interaction with RAB10, an unexplored target in HCC treatment. Looking ahead, the proposed direction requires experimental validation to confirm the computational predictions and further establish the efficacy of Amentoflavone in inhibiting RAB10 and suppressing HCC progression. In addition, off-target analysis and strategies to further enhance its PK properties should be key areas of future research. Moreover, continued research should explore its potential synergies with existing therapeutic strategies, as well as its applicability in other cancers where RAB10 overexpression contributes to disease progression.

Acknowledgement

The authors are grateful to the Research cell of Noakhali Science and Technology University and Ministry of Science and Technology, Bangladesh, for financial support. The authors also acknowledge the use of several computational tools and databases

that supported various aspects of this study. Molecular visualization and analysis were performed using PyMOL and Discovery Studio. Molecular dynamics simulation results were analyzed using the YASARA Molecular Dynamics Trajectory Analysis tool. 3D conformer of the ligands was retrieved from the PubChem Database.

Data Availability Statement

The data that support this work are available upon reasonable request to the corresponding author. The final outputs of all the analyses are documented in the main manuscript.

Ethical Statement

This study does not contain any studies with human or animal subjects performed by any of the authors.

Conflicts of Interest

The authors declare that they have no conflicts of interest to this work.

Author Contribution Statement

Md. Anayet Ullah: Methodology, Software, Formal analysis, Writing—original draft, Visualization. Priya Paul: Software, Formal analysis, Writing—original draft, Visualization. Sadia Afrin Runa: Formal analysis, Writing—original draft. Fatema Tuz Johura: Formal analysis, Writing—original draft. Mahafujul Islam Quadery Tonmoy: Conceptualization, Methodology, Software, Validation, Formal analysis, Writing—review & editing, Visualization. Md. Shahriar Kabir Shakil: Resources, Writing—review & editing. Rumana Rashid: Writing—review & editing. Md. Mizanur Rahaman: Resources, Writing—review & editing. Newaz Mohammed Bahadur: Conceptualization, Validation, Investigation, Resources, Writing—review & editing, Supervision.

References

- [1] Ker, C. G., Chen, J. L., & Chen, Y. S. (2023). Trends of treatments of hepatocellular carcinoma in recent 3-decade based on the top-100 influential articles from Taiwan. E-Da Medical Journal, 10(4), 34–46. https://doi.org/10.6966/ EDMJ.202312_10(4).0004
- [2] Nakano, M., Yatsuhashi, H., Bekki, S., Takami, Y., Tanaka, Y., Yoshimaru, Y., ..., & Torimura, T. (2022). Trends in hepatocellular carcinoma incident cases in Japan between 1996 and 2019. *Scientific Reports*, 12(1), 1517. https://doi.org/10.1038/s41598-022-05444-z
- [3] Schulte, L. A., López-Gil, J. C., Sainz, B., & Hermann, P. C. (2020). The cancer stem cell in hepatocellular carcinoma. *Cancers*, 12(3), 684. https://doi.org/10.3390/cancers12030684
- [4] Mašulović, D., Igić, A., Filipović, A., Zakošek, M., Bulatović, D., Mijović, K., ..., & Galun, D. (2023). A rare case of isolated hepatocellular carcinoma metastasis in left mandibular region in a patient with hepatitis C virus liver cirrhosis diagnosed after the onset of COVID-19 infection. *Medicina*, 59(11), 1992. https://doi.org/10.3390/medicina59111992
- [5] Wang, W., Jia, W. D., Hu, B., & Pan, Y. Y. (2017). RAB10 overexpression promotes tumor growth and indicates poor prognosis of hepatocellular carcinoma. *Oncotarget*, 8(16), 26434–26447. https://doi.org/10.18632/oncotarget.15507
- [6] Helal, I. M., Kamal, M. A., Abd El-Aziz, M. K., & El Tayebi, H. M. (2024). Epigenetic tuning of tumour-associated

- macrophages (TAMs): A potential approach in hepatocellular carcinoma (HCC) immunotherapy. *Expert Reviews in Molecular Medicine*, *26*, e18. https://doi.org/10.1017/erm. 2024.9
- [7] Gordan, J. D., Kennedy, E. B., Abou-Alfa, G. K., Beg, M. S., Brower, S. T., Gade, T. P., ..., & Rose, M. G. (2020). Systemic therapy for advanced hepatocellular carcinoma: ASCO guideline. *Journal of Clinical Oncology*, 38(36), 4317–4345. https://doi.org/10.1200/JCO.20.02672
- [8] Kamal, M. A., Mandour, Y. M., Abd El-Aziz, M. K., Stein, U., & El Tayebi, H. M. (2022). Small molecule inhibitors for hepatocellular carcinoma: Advances and challenges. *Molecules*, 27(17), 5537. https://doi.org/10.3390/molecules27175537
- [9] Lee, Y. T., Tan, Y. J., & Oon, C. E. (2018). Molecular targeted therapy: Treating cancer with specificity. *European Journal of Pharmacology*, 834, 188–196. https://doi.org/10.1016/j.ejphar. 2018.07.034
- [10] Xie, Y. H., Chen, Y. X., & Fang, J. Y. (2020). Comprehensive review of targeted therapy for colorectal cancer. *Signal Transduction and Targeted Therapy*, 5(1), 22. https://doi.org/ 10.1038/s41392-020-0116-z
- [11] Cogdill, A. P., Prieto, P. A., Reuben, A., & Wargo, J. A. (2017). Gene targeting meets cell-based therapy: Raising the tail, or merely a whimper? *Clinical Cancer Research*, 23(2), 327–329. https://doi.org/10.1158/1078-0432.CCR-16-2493
- [12] Zaher, A., Petronek, M. S., Allen, B. G., & Mapuskar, K. A. (2024). Balanced duality: H₂O₂-based therapy in cancer and its protective effects on non-malignant tissues. *International Journal of Molecular Sciences*, 25(16), 8885. https://doi.org/ 10.3390/ijms25168885
- [13] Cheng, X., Wu, C., Xu, H., Zou, R., Li, T., & Ye, S. (2024). miR-557 inhibits hepatocellular carcinoma progression through Wnt/β-catenin signaling pathway by targeting RAB10. *Aging*, 16(4), 3716–3733. https://doi.org/10.18632/aging.205554
- [14] Isabella, A. J., & Horne-Badovinac, S. (2016). Rab10-mediated secretion synergizes with tissue movement to build a polarized basement membrane architecture for organ morphogenesis. *Developmental Cell*, 38(1), 47–60. https://doi.org/10.1016/j. devcel.2016.06.009
- [15] Vieira, O. V. (2018). Rab3a and Rab10 are regulators of lysosome exocytosis and plasma membrane repair. *Small GTPases*, *9*(4), 349–351. https://doi.org/10.1080/21541248.2016.1235004
- [16] Yang, C. C., Meng, G. X., Dong, Z. R., & Li, T. (2021). Role of Rab GTPases in hepatocellular carcinoma. *Journal of Hepatocellular Carcinoma*, 8, 1389–1397. https://doi.org/10. 2147/JHC.S336251
- [17] Zhang, Y. J., Pan, Q., Yu, Y., & Zhong, X. P. (2020). microRNA-519d induces autophagy and apoptosis of human hepatocellular carcinoma cells through activation of the AMPK signaling pathway via Rab10. *Cancer Management and Research*, 12, 2589–2602. https://doi.org/10.2147/CMAR.S207548
- [18] Lengauer, T. (2002). Bioinformatics—From genomes to drugs. USA: Wiley-VCH. https://doi.org/10.1002/3527601481
- [19] Matin, M. M., Chakraborty, P., Alam, M. S., Islam, M. M., & Hanee, U. (2020). Novel mannopyranoside esters as sterol 14α-demethylase inhibitors: Synthesis, PASS predication, molecular docking, and pharmacokinetic studies. *Carbohydrate Research*, 496, 108130. https://doi.org/10.1016/j.carres.2020.108130
- [20] Du, X., Li, Y., Xia, Y. L., Ai, S. M., Liang, J., Sang, P., ..., & Liu, S. Q. (2016). Insights into protein–ligand interactions: Mechanisms, models, and methods. *International Journal of Molecular Sciences*, 17(2), 144. https://doi.org/10.3390/ijms17020144

- [21] Jian, Y., He, Y., Yang, J., Han, W., Zhai, X., Zhao, Y., & Li, Y. (2018). Molecular modeling study for the design of novel peroxisome proliferator-activated receptor gamma agonists using 3D-QSAR and molecular docking. *International Journal of Molecular Sciences*, 19(2), 630. https://doi.org/10.3390/ijms19020630
- [22] Akhtar, A., Amir, A., Hussain, W., Ghaffar, A., & Rasool, N. (2019). In silico computations of selective phytochemicals as potential inhibitors against major biological targets of diabetes mellitus. *Current Computer-Aided Drug Design*, 15(5), 401–408. https://doi.org/10.2174/1573409915666190130164923
- [23] Naithani, U., & Guleria, V. (2024). Integrative computational approaches for discovery and evaluation of lead compound for drug design. Frontiers in Drug Discovery, 4, 1362456. https://doi.org/10.3389/fddsv.2024.1362456
- [24] Vardhan, S., & Sahoo, S. K. (2020). *In silico* ADMET and molecular docking study on searching potential inhibitors from limonoids and triterpenoids for COVID-19. *Computers in Biology and Medicine*, *124*, 103936. https://doi.org/10.1016/j.compbiomed.2020.103936
- [25] Yalcin, S. (2020). Molecular docking, drug likeness, and ADMET analyses of passiflora compounds as P-glycoprotein (P-gp) inhibitor for the treatment of cancer. *Current Pharmacology Reports*, 6(6), 429–440. https://doi.org/10.1007/s40495-020-00241-6
- [26] Tonmoy, M. I. Q., Ahmed, S. F., Hami, I., Shakil, M. S. K., Verma, A. K., Hasan, M., ..., & Hossain, M. S. (2022). Identification of novel inhibitors of high affinity iron permease (FTR1) through implementing pharmacokinetics index to fight against black fungus: An *in silico* approach. *Infection, Genetics and Evolution, 106*, 105385. https://doi.org/10.1016/j.meegid.2022.105385
- [27] Burley, S. K., Bhikadiya, C., Bi, C., Bittrich, S., Chen, L., Crichlow, G. V., ..., & Zhuravleva, M. (2021). RCSB protein data bank: Powerful new tools for exploring 3D structures of biological macromolecules for basic and applied research and education in fundamental biology, biomedicine, biotechnology, bioengineering and energy sciences. *Nucleic Acids Research*, 49(D1), D437–D451. https://doi.org/10.1093/nar/gkaa1038
- [28] Rai, A., Oprisko, A., Campos, J., Fu, Y., Friese, T., Itzen, A., ..., & Müller, M. P. (2016). bMERB domains are bivalent Rab8 family effectors evolved by gene duplication. *Elife*, 5, e18675. https://doi.org/10.7554/eLife.18675
- [29] da Fonseca, A. M., Caluaco, B. J., Madureira, J. M. C., Cabongo, S. Q., Gaieta, E. M., Djata, F., ..., & Marinho, E. S. (2024). Screening of potential inhibitors targeting the main protease structure of SARS-CoV-2 via molecular docking, and approach with molecular dynamics, RMSD, RMSF, H-Bond, SASA and MMGBSA. *Molecular Biotechnology*, 66(8), 1919–1933. https://doi.org/10.1007/s12033-023-00831-x
- [30] Alam, R., Rahman, G. S., Hasan, N., & Chowdhury, A. S. (2020). A De-Novo drug design and ADMET study to design small molecule stabilisers targeting mutant (V210I) human prion protein against familial Creutzfeldt-Jakob disease (fCJD). *International Journal* of Computational Biology and Drug Design, 13(1), 21–35. https://doi.org/10.1504/IJCBDD.2020.105103
- [31] Kelley, L. A., Mezulis, S., Yates, C. M., Wass, M. N., & Sternberg, M. J. E. (2015). The Phyre2 web portal for protein modeling, prediction and analysis. *Nature Protocols*, 10(6), 845–858. https://doi.org/10.1038/nprot.2015.053
- [32] Kannan, C., Radhakrishnan, S., Sambathkumar, R., Dhanaraja, D., Muvendhiran, S., & Dharnisha, N. J. (2024). A review on

- step into the future: Python prescription (PyRx) transforms virtual drug discovery with AI-driven tools. *African Journal of Biomedical Research*, 27(3S), 790–795. https://doi.org/10.53555/AJBR.v27i3S.2119
- [33] Dallakyan, S., & Olson, A. J. (2015). Small-molecule library screening by docking with PyRx. In J. E. Hempel, C. H. Williams, & C. C. Hong (Eds.), *Chemical biology: Methods and protocols* (pp. 243–250). Springer. https://doi.org/10.1007/978-1-4939-2269-7_19
- [34] Kondapuram, S. K., Sarvagalla, S., & Coumar, M. S. (2021). Docking-based virtual screening using PyRx tool: Autophagy target Vps34 as a case study. In M. S. Coumar (Ed.), Molecular docking for computer-aided drug design: Fundamentals, techniques, resources and applications (pp. 463–477). Academic Press. https://doi.org/10.1016/B978-0-12-822312-3.00019-9
- [35] Daina, A., Michielin, O., & Zoete, V. (2017). SwissADME: A free web tool to evaluate pharmacokinetics, drug-likeness and medicinal chemistry friendliness of small molecules. *Scientific Reports*, 7(1), 42717. https://doi.org/10.1038/srep42717
- [36] Bickerton, G. R., Paolini, G. V., Besnard, J., Muresan, S., & Hopkins, A. L. (2012). Quantifying the chemical beauty of drugs. *Nature Chemistry*, 4(2), 90–98. https://doi.org/10.1038/nchem.1243
- [37] Lipinski, C. A., Lombardo, F., Dominy, B. W., & Feeney, P. J. (2012). Experimental and computational approaches to estimate solubility and permeability in drug discovery and development settings. *Advanced Drug Delivery Reviews*, 64, 4–17. https://doi.org/10.1016/j.addr.2012.09.019
- [38] Pantaleão, S. Q., Fernandes, P. O., Gonçalves, J. E., Maltarollo, V. G., & Honorio, K. M. (2022). Recent advances in the prediction of pharmacokinetics properties in drug design studies: A review. *ChemMedChem*, *17*(1), e202100542. https://doi.org/10.1002/cmdc.202100542
- [39] Inamdar, A., Pote, S., Sawant, S., Salve, P. S., Suryawanshi, S. S., & Palled, M. (2023). Physicochemical and pharmacokinetic properties' screening of selected cardiovascular agents: An insilico approach. Research Square. https://doi.org/10.21203/rs.3. rs-2653667/v1
- [40] Pires, D. E., Blundell, T. L., & Ascher, D. B. (2015). pkCSM: Predicting small-molecule pharmacokinetic and toxicity properties using graph-based signatures. *Journal of Medicinal Chemistry*, 58(9), 4066–4072. https://doi.org/10. 1021/acs.jmedchem.5b00104
- [41] Ahmad, S., Waheed, Y., Ismail, S., Bhatti, S., Abbasi, S. W., & Muhammad, K. (2021). Structure-based virtual screening identifies multiple stable binding sites at the RecA domains of SARS-CoV-2 helicase enzyme. *Molecules*, 26(5), 1446. https://doi.org/10.3390/molecules26051446
- [42] Hosen, M. A., El Bakri, Y., Rehman, H. M., Hashem, H. E., Saki, M., & Kawsar, S. M. A. (2024). A computational investigation of galactopyranoside esters as antimicrobial agents through antiviral, molecular docking, molecular dynamics, pharmacokinetics, and bioactivity prediction. *Journal of Biomolecular Structure and Dynamics*, 42(2), 1015–1030. https://doi.org/10.1080/07391102.2023.2198606
- [43] Salo-Ahen, O. M. H., Alanko, I., Bhadane, R., Bonvin, A. M. J. J., Honorato, R. V., Hossain, S., ..., & Vanmeert, M. (2021). Molecular dynamics simulations in drug discovery and pharmaceutical development. *Processes*, 9(1), 71. https://doi.org/10.3390/pr9010071
- [44] Land, H., & Svedendahl Humble, M. (2018). YASARA: A tool to obtain structural guidance in biocatalytic investigations.

- In U. T. Bornscheuer & M. Höhne (Eds.), *Protein engineering: Methods and protocols* (pp. 43–67). Springer. https://doi.org/10.1007/978-1-4939-7366-8_4
- [45] Krieger, E., Dunbrack, R. L., Hooft, R. W. W., & Krieger, B. (2012). Assignment of protonation states in proteins and ligands: Combining pK_a prediction with hydrogen bonding network optimization. In R. Baron (Ed.), *Computational drug discovery and design* (pp. 405–421). Springer. https://doi.org/10.1007/978-1-61779-465-0_25
- [46] Chubak, I., Scalfi, L., Carof, A., & Rotenberg, B. (2021). NMR relaxation rates of quadrupolar aqueous ions from classical molecular dynamics using force-field specific Sternheimer factors. *Journal of Chemical Theory and Computation*, 17(10), 6006–6017. https://doi.org/10.1021/acs.jctc.1c00690
- [47] Case, D. A., Aktulga, H. M., Belfon, K., Ben-Shalom, I. Y., Berryman, J. T., Brozell, S. R., ..., & Kollman, P. A. (2023). Amber 2023: Reference manual. USA: University of California.
- [48] Bhrdwaj, A., Abdalla, M., Pande, A., Madhavi, M., Chopra, I., Soni, L., ..., & Singh, S. K. (2023). Structure-based virtual screening, molecular docking, molecular dynamics simulation of EGFR for the clinical treatment of glioblastoma. *Applied Biochemistry and Biotechnology*, 195(8), 5094–5119. https://doi.org/10.1007/s12010-023-04430-z
- [49] Shakil, S., Rizvi, S. M. D., & Greig, N. H. (2021). High throughput virtual screening and molecular dynamics simulation for identifying a putative inhibitor of bacterial CTX-M-15. Antibiotics, 10(5), 474. https://doi.org/10.3390/ antibiotics10050474
- [50] de Souza, B. C., Lacerda, P. S., Silva da Rocha Pita, S., Kato, R. B., & Leite, F. H. A. (2021). Identification of potential *Leishmania chagasi* superoxide dismutase allosteric modulators by structure-based computational approaches: Homology modelling, molecular dynamics and pharmacophore-based virtual screening. *Journal of Biomolecular Structure and Dynamics*, 39(18), 7000–7016. https://doi.org/10.1080/07391102.2020.1804453
- [51] Cabrera, N., Cuesta, S. A., Mora, J. R., Paz, J. L., Márquez, E. A., Espinoza-Montero, P. J., ..., & Contreras-Torres, E.

- (2022). Searching glycolate oxidase inhibitors based on QSAR, molecular docking, and molecular dynamic simulation approaches. *Scientific Reports*, *12*(1), 19969. https://doi.org/10.1038/s41598-022-24196-4
- [52] Nabi, F., Ahmad, O., Ali Khan, Y., Nabi, A., Hashmi, M. A., Abul Qais, F., ..., & Khan, R. H. (2022). Computational studies on phylogeny and drug designing using molecular simulations for COVID-19. *Journal of Biomolecular Structure and Dynamics*, 40(21), 10753–10762. https://doi.org/10.1080/07391102.2021.1947895
- [53] Irsal, R. A. P., Gholam, G. M., Firdaus, D. A., Liwanda, N., & Chairunisa, F. (2024). Molecular docking and dynamics of Xylocarpus granatum as a potential Parkinson's drug targeting multiple enzymes. *Borneo Journal of Pharmacy*, 7(2), 161–171. https://doi.org/10.33084/bjop.v7i2.6810
- [54] Kimura, Y., Ito, H., Ohnishi, R., & Hatano, T. (2010). Inhibitory effects of polyphenols on human cytochrome P450 3A4 and 2C9 activity. Food and Chemical Toxicology, 48(1), 429–435. https:// doi.org/10.1016/j.fct.2009.10.041
- [55] Lee, K. C., Chen, W. T., Liu, Y. C., Lin, S. S., & Hsu, F. T. (2018). Amentoflavone inhibits hepatocellular carcinoma progression through blockage of ERK/NF-κB activation. *In Vivo*, 32(5), 1097–1103. https://doi.org/10.21873/invivo. 11351
- [56] Chen, W. L., Hsieh, C. L., Chen, J. H., Huang, C. S., Chen, W. T., Kuo, Y. C., ..., & Hsu, F. T. (2017). Amentoflavone enhances sorafenib-induced apoptosis through extrinsic and intrinsic pathways in sorafenib-resistant hepatocellular carcinoma SK-Hep1 cells *in vitro*. *Oncology Letters*, 14(3), 3229–3234. https://doi.org/10.3892/ol.2017.6540

How to Cite: Ullah, M. A., Paul, P., Runa, S. A., Johura, F. T., Tonmoy, M. I. Q., Shakil, M. S. K., . . . , & Bahadur, N. M. (2025). Computer-Aided Drug Design Identifies Amentoflavone as Novel RAB10 Inhibitor: Unlocking New Horizons in Hepatocellular Carcinoma Therapy. *Medinformatics*, 2(4), 288–298. https://doi.org/10.47852/bonviewMEDIN52024568